We are IntechOpen, the world's leading publisher of Open Access books Built by scientists, for scientists

4,800
Open access books available

122,000
International authors and editors

135M
Downloads

Our authors are among the

154
Countries delivered to

TOP 1%
most cited scientists

12.2%
Contributors from top 500 universities

CLARIVATE ANALYTICS BOOK CITATION INDEX INDEXED

WEB OF SCIENCE™

Selection of our books indexed in the Book Citation Index in Web of Science™ Core Collection (BKCI)

Interested in publishing with us?
Contact book.department@intechopen.com

Numbers displayed above are based on latest data collected.
For more information visit www.intechopen.com

1

Q-Switching with Single Crystal Photo-Elastic Modulators

F. Bammer[1], T. Schumi[1], J. R. Carballido Souto[1], J. Bachmair[1],
D. Feitl[2], I. Gerschenson[2], M. Paul[2] and A. Nessmann[2]
[1]*Vienna University of Technology*
[2]*Gymnasium Stubenbastei, Vienna*
Austria

1. Introduction

Q-switching is a common technology to produce laser pulses. It is based on a fast optical switch in the laser resonator blocking laser light while pumping energy is stored in the gain medium. Usually electro- or acousto-optic Q-switches are used for this task. We introduce here Single Crystal Photo-Elastic Modulators (SCPEM) that combine features of both technologies, namely first the change of polarization in case of electro-optics, and second the use of the photo-elastic effect as in acousto-optics. These resonant devices allow running lasers on a constant pulse repetition frequency determined by the crystal size and excited eigenmode.

2. Photo-elastic modulators

We will give here an overview about the basics and theory of Photo-Elastic Modulators (PEM). This will include information about classical PEM excited, from the end, from the sides, and from two sides. Then we will describe single crystal photo-elastic modulators with focus on the material from the crystal symmetry group 3m and short discussion of other groups.

2.1 Conventional photo-elastic modulators

Conventional photo-elastic modulators (PEMs, Fig. 1, left) modulate the polarization of a light beam and are mainly used in ellipsometry in the form of Kemp-modulators (Kemp, 1969; Kemp, 1987; www.hindsinstruments.com). They are made of a piece of optical glass which is glued to a quartz-crystal. Both pieces are adjusted to have the same longitudinal resonance frequency. When the quartz-crystal is electrically excited with the proper frequency the system will start a strong resonant oscillation. Since damping is low the strain amplitudes become even at low voltage amplitudes so large that a significant artificial birefringence modulation due to the photo-elastic effect is caused. Polarized light passing the glass will experience a strong modulation of its polarization.
A more advanced modulator is shown in the middle of Fig. 1 which is used for the infrared, where due to the longer wavelengths strong retardation is required, usually with ZnSe or

GaAs as the optical material. Its special shape allows together with the two actuators a superposition of a vertical and horizontal longitudinal mode.
Further Canit & Badoz (1983) proposed an advanced design for a conventional PEM, where small actuators are glued on the sides of the glass piece (Fig. 1, right) to excite the 3rd harmonics of the longitudinal horizontal mode.

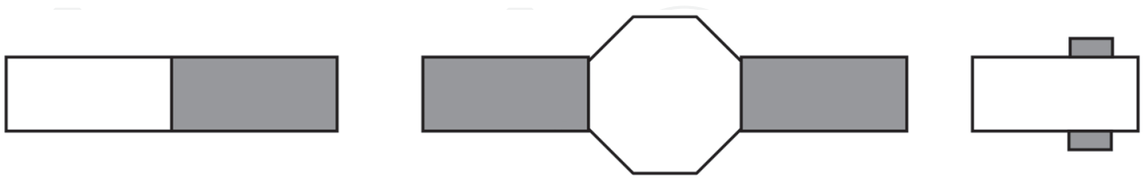

Fig. 1. Different shapes of classical photo-elastic modulators. The actuators are shown grey.

Disadvantages of conventional PEMs are:
- High precision is needed to adjust the system such that it oscillates with high merit.
- Furthermore the device is very large compared to its useful aperture.
- No superposition of frequency adjusted higher modes is possible
- the gluing process of the actuator(s) can lead to stresses in the glass and hence to an unwanted stray birefringence

2.2 Definition and description of a SCPEM

A Single Crystal Photo-Elastic Modulator (SCPEM, Fig. 1) is a piezoelectric optical transparent crystal that is electrically excited on one of its resonance frequencies. Many possible configurations are described by Bammer (2007).

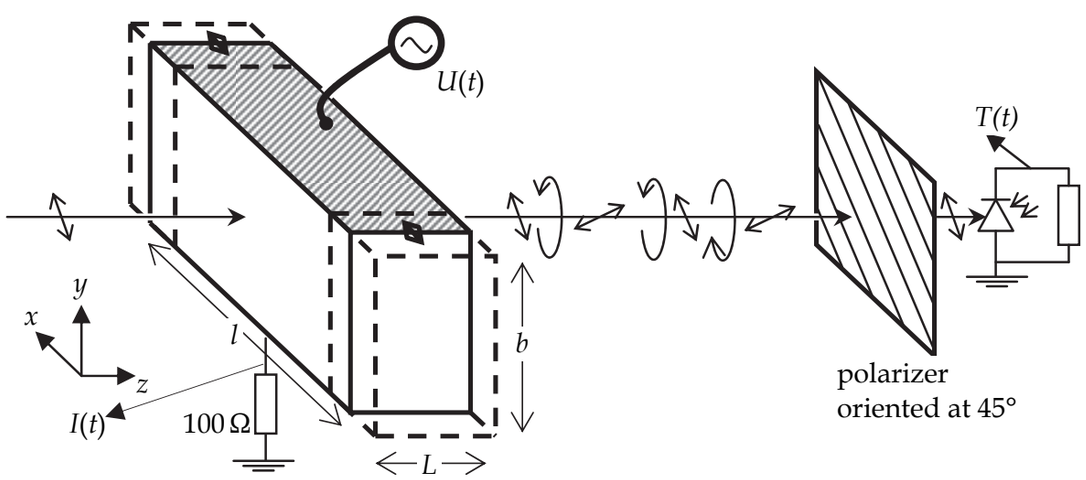

Fig. 2. Single Crystal Photo-Elastic Modulator made of a 3m-crystal (Bammer, 2009).

A necessary feature is that the polarization of light of any wavelength passing this crystal must not be changed when the crystal is at rest. This for example cannot be fulfilled with the quartz crystal of a conventional PEM, due to its optical activity (Nye, 1985), which would need to be compensated by a second reversely oriented quartz crystal as proposed in an early patent on PEMs (n.n., 1925).

SCPEMs for the MIR are based on 43m crystals and are experimentally and theoretically described by Weil & Halido (1974). Fig. 2 shows now one favourable configuration based on a crystal with symmetry 3m.
The light travels along the optical axis (= z-axis), the exciting electrical field points into the y-direction, and in most cases the longitudinal x-eigenmode is used. Two further important eigenmodes are the longitudinal y-eigenmode and the shear yz-eigenmode. Of course there exist infinitely many higher eigen-modes and frequencies.
In most cases a polarizer (analyzer) oriented at 45° is placed behind the modulator. Fig. 2 further shows a photo diode to get a transmission signal T and a resistor (here with 100 Ω) to generate a measure for the piezo electric current I generated by the crystal.

2.2.1 Use as a Q-switch

We define now for monochromatic light with the wavelength λ the retardation as

$$\delta = 2\pi \frac{L\,(n_x - n_y)}{\lambda} \tag{1}$$

where L is the z-dimension of the crystal and n_x, n_y are the refractive indices for x- and y-polarized light. They are calculated in chapter 2.2 for the photo-elastic effect and in chapter 2.6 for the electro-optic effect.

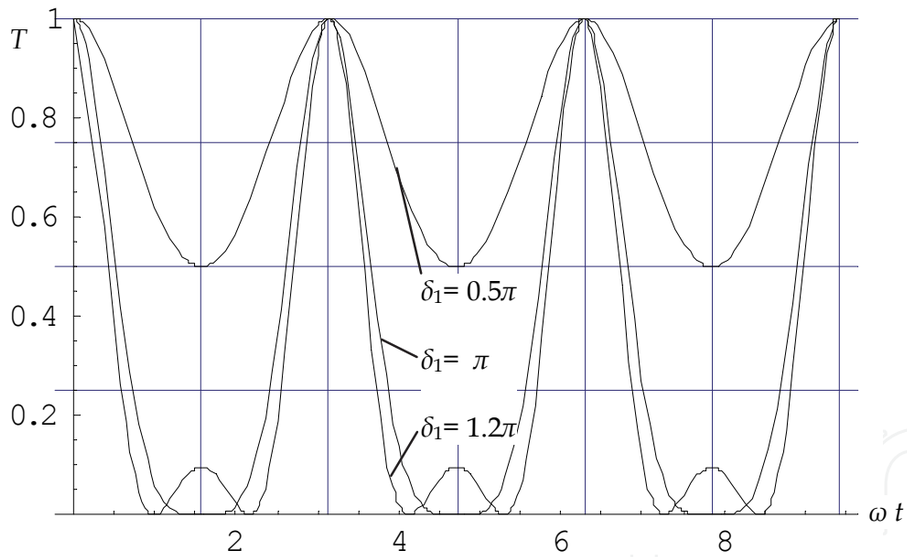

Fig. 3. Transmission curves for the configuration in Fig. 2.

The transmission $T(\delta)$ for the situation of Fig. 2 is

$$T(\delta) = T_{min} + (T_{max} - T_{min}) \cos^2(\delta/2) = T_{min} + (T_{max} - T_{min})\,(1 + \cos\delta)/2\,. \tag{2}$$

The parameters T_{min} and T_{max} take into account that in reality no perfect optical "on" or "off" is possible. For the discussion in this chapter we set $T_{min} = 0$ and $T_{max} = 1$ and the Eq. 2 will reduce to the theoretical formulas found in elementary books like Bass, (1995) or Maldonado, (1995).
Based on Eq. (2) and with a retardation course

$$\delta(t) = \delta_1 \sin(\omega t) \tag{3}$$

transmission courses as depicted in Fig. 3 can be realized (ω… angular frequency of one resonance).
The choice $\delta_1 = \pi$ leads to quite sharp transmission peaks, while during the off-time a second peak with ~10% transmission evolve. When this is used for Q-switching it can be expected that the small off-transmission will not lead to an emission while the sharp transmission peaks will cause defined pulsing of the laser. This was first demonstrated for a low power fibre laser (Bammer & Petkovsek, 2007). For high gain lasers however this will not longer work, typical problems like pre-/post-lasing or spiking are encountered, and a second eigenmode must be added to get even sharper transmission peaks as discussed later.

2.2.2 Retardation control

Fig. 4 shows typical resonance curves of crystal-current and crystal-deformation (e.g. the movement of one x-facet or the angle of the z-facet in case of a shear-mode) at any (well working) resonance frequency.

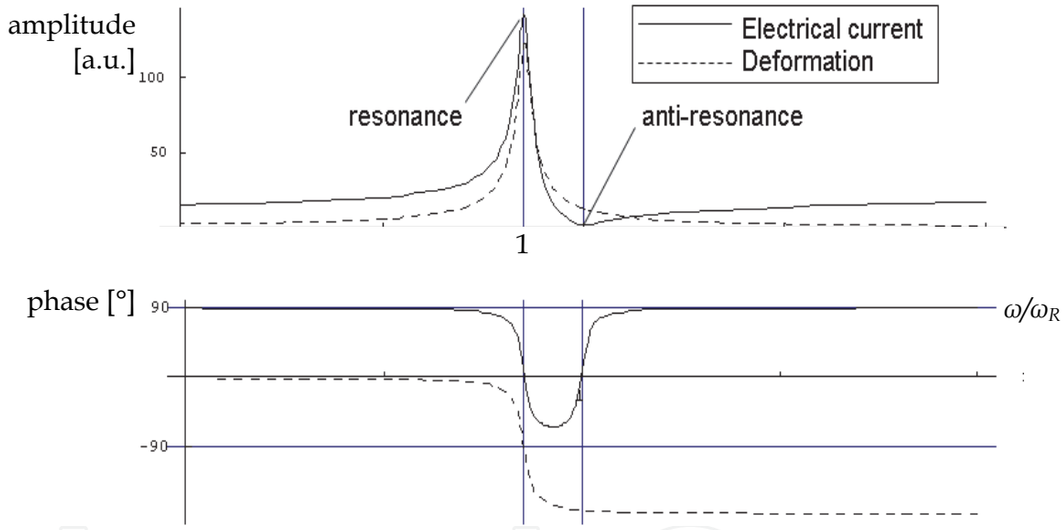

Fig. 4. Typical resonance curves of a piezo crystal for current and deformation

One important fact here is that the relation between deformation and current is approximately constant within the FWHM-resonance bandwidth (usually in the range 1/1000-1/10000 of the resonance frequency). In fact it changes linearly with the frequency, but since the frequency change is so small within the bandwidth and since the modulator is not useful outside of this bandwidth, a constant value can be assumed. For Q-switching this is sufficiently precise, for other applications, e.g. ellipsometry more accuracy is needed.
The reason why we point out this relation between current and deformation, which is directly connected to the retardation[1], is the following: The crystal frequency and the damping can change during operation, e.g. when the crystal heats up, expands and has then

[1] This is only true if the electro-optic effect is neglected, which can be safely done since the usual PEM-voltage-amplitudes in the order of ~10V are much lower than the kilo-Volts needed for a measureable electro-optic effect.

increased contact and damping forces with the contacts. Since this directly influences the relation between voltage amplitude and retardation amplitude, it is better to track and control the current amplitude during in order to keep the retardation amplitude on a desired value. (Bammer, 2007; Bammer & Petkovsek 2011) give formulas for the calculation of these relations with ~10% accuracy, such that practically one has to measure the real values anyway. Typically the retardation per current of the most used material for SCPEM, namely $LiTaO_3$, is around 50nm/mA corresponding to ~0.5rad/mA for λ = 632nm.
Regard that not al 3m-materials will show the x-oscillation discussed now. For BBO it seems that this x-oscillation cannot be excited (Bammer & Petkovsek 2011), where only a yz-shear-eigenmode seems to work (Fig. 6), due to its degenerated elasticity matrix.

2.2.3 Dual mode operation

Besides the x-eigenmode sketched in Fig. 2 a y-excitation can also excite longitudinal y-modes and shear yz-modes. In case of the y-modes different shapes are found corresponding to different acoustic waveguide modes (Dieulesaint & Royer, 2000). E.g. for a $LiTaO_3$-crystal with the dimensions 28x9.5x4mm Fig. 5 shows two different y-eigenmodes at the frequencies 258.8 kHz and 273.2 kHz. The higher mode shows additionally a strong xy-shear component.

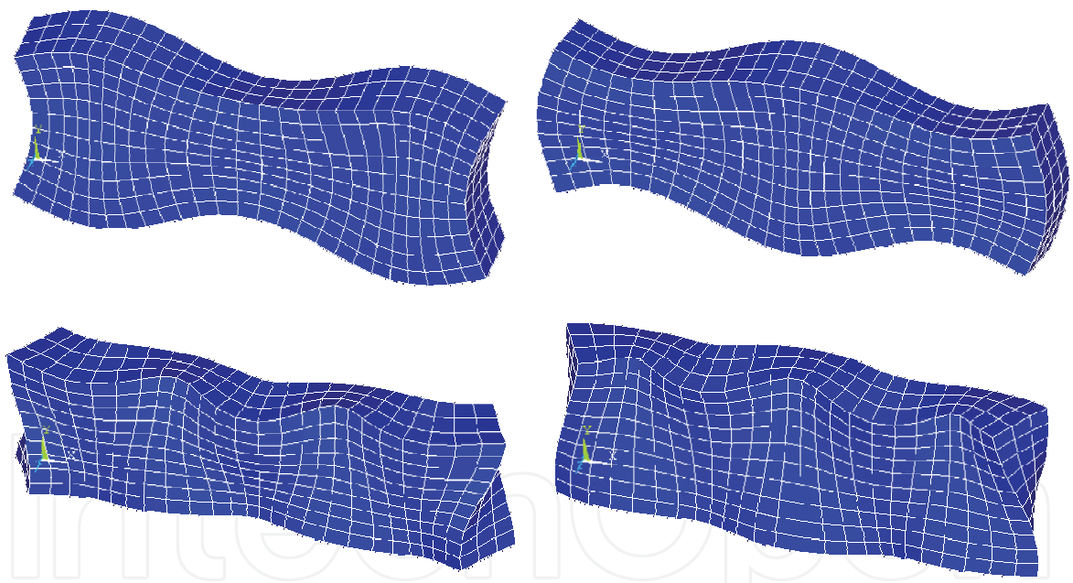

Fig. 5. ANSYS-simulation: y-eigenmode of a y-excited $LiTaO_3$-crystal with dimension 28.8x9.5x4mm with two knots at 258.8 kHz (upper pictures) and with four knots at 273.2 kHz (lower pictures). The real measured values were for one sample (out of five with all slightly different eigenfrequencies) 260.62 kHz and 275.86 kHz.

Eigenmodes as shown in Fig. 5 can now be superposed to the x-oscillation. This makes sense if the higher frequency is exactly three times higher than the basic frequency. Here "exact" means that the 3x-multiple of the basic frequency must be within the FWHM-bandwidth of the higher frequency. For the crystal simulated in Fig. 5 it was possible to tune the first harmonic from initially 90.8 kHz to 91.4 kHz by grinding the x-length from initially 28.8mm

to 28.6mm, such that the frequency was one third of the eigen-frequency 274.2 kHz (Petkovsek et. al. 2011).
Fig. 6 shows as a further example the yz-shear mode of a y-excited BBO-crystal with dimensions 8.6 x 4.05 x 4.5mm at 131.9 kHz (Bammer & Petkovsek, 2011). A similar mode is also possible for $LiTaO_3$ and in (Bammer & Petkovsek, 2008) a dual mode operation of a LiTaO3-crystal (21x7x5mm) with the yz-shear mode (381kHz) and the x-mode (127kHz) was demonstrated.
We remark that dual mode operation was also proposed for conventional PEMs by Canit & Pichon, C., 1984, but without the possibility of frequency tuning, as given for SCPEMs.

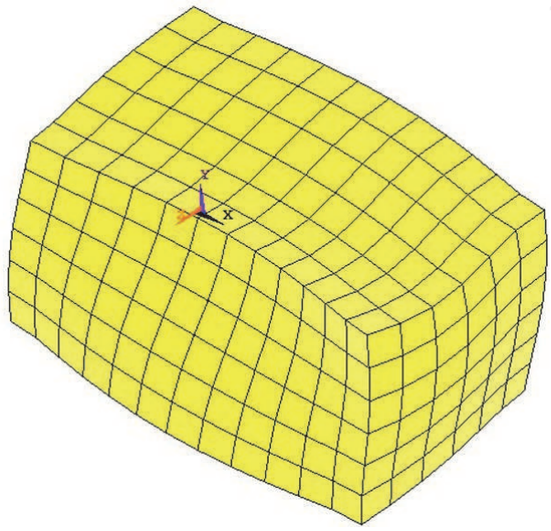

Fig. 6. ANSYS-simulation: yz-shear-eigenmode with 122.85 kHz of a y-excited BBO-crystal with dimensions 8.6 x 4.05 x 4.5mm

What can be now achieved by adding a second frequency-tuned eigenmode? The retardation in Eq. 3 is now modified according to

$$\delta(t) = \delta_1 \sin(\omega t) + \delta_3 \sin(3\,\omega t) \tag{4}$$

For this optimized result the series in Eq. 4 must approximate a square wave function oscillating between $-\pi$ and $+\pi$ yielding the values $\delta_1 = 4$, $\delta_3 = 4/3$. With this inserted in Eq. 2 the transmission course as depicted in Fig. 7 (in comparison with two curves $\delta_1 = \pi$, $\delta_3 = 0$; $\delta_1 = 1.2\pi$, $\delta_3 = 0$ from Fig. 3) can be produced.
Table 1 shows a comparison of the different transmission widths and rise times for the three transmission curves shown in Fig. 7. The values are given first in % of the period time of the base oscillation and second in ns for the 91.4kHz-crystal shown in Fig. 5.

δ_1	δ_3	FWHM-width [%]	FWHM-width [ns]@91.4kHz	Rise-time [%]	Rise-time [ns]@91.4kHz
π	0	16.7	1823	11.3	1241
1.2π	0	13.7	1497	8.8	962
4	4/3	6.5	708	4.2	460

Table 1. FWHM-transmission widths and rise times for a dual mode SCPEM

The proper addition of a second mode decrease transmission width and rise time by a factor of more than 2.

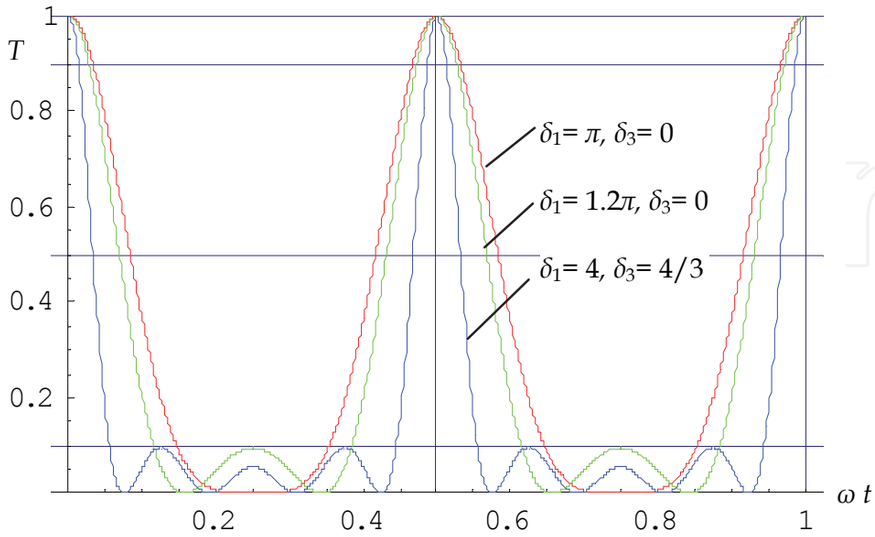

Fig. 7. Transmission curves of a dual mode SCPEM with $\delta_1 = \pi$, $\delta_3 = 0$; $\delta_1 = 1.2\pi$, $\delta_3 = 0$; and $\delta_1 = 4$, $\delta_3 = 4/3$.

3. Simulating SCPEM-Q-switching

In this chapter a simple numerical model for the description of the laser dynamics will be introduced and applied to a Nd:YAG-rod laser.

3.1 The laser photon life time t_p

The life-time t_p of a photon in a laser cavity with intrinsic transmission T_c, outcoupler reflection R_{out}, modulated internal transmission $T(t)$ and roundtrip frequency f_c is given by

$$t_p(t) = -1 \Big/ \ln\left(T_c\, R_{out}\, T(t)\right)^{f_c} \tag{5}$$

If the internal transmission is due to a SCPEM with transmission course as in Fig. 7, then a strong modulation of the photon life time t_p is produced. This parameter is of utmost importance in the laser rate equations describing the laser dynamics.

3.2 The laser rate equations

The simplest model to describe laser-activity is based on two coupled rate equations for the average population density n (of the upper laser level) and the average photon density P in the laser gain medium (see for an introduction e.g. Siegmann, 1986).

$$\begin{aligned} \dot{P}(t) &= \Gamma\, c\, \sigma\, P(t)\left(n(t) - n_{th}\right) - P(t) / t_p(t) + M\, n(t) / t_n \\ \dot{n}(t) &= p\left(1 - n(t) / n_{\max}\right) - n(t) / t_n - c\, \sigma\, P(t)\left(n(t) - n_{th}\right) \end{aligned} \tag{6}$$

with c…velocity of light in the gain medium, σ…cross-section of induced emission, M…fraction of light emitted by spontaneous emission which travels in a direction that

contributes to the laser mode by ASE (amplified spontaneous emission) and is also responsible for the start of laser operation, t_n…life time of the upper laser level, $p = P_{abs}/E_{pp}/V_g$ (P_{abs}…absorbed pumping power, E_{pp}…pump photon energy, V_g…volume of gain medium) … pumping rate when the upper laser level is empty (number of excited states per m³ and s), p (1 - n(t)/n_{max})… reduced pumping rate when the upper laser level becomes filled using n_{max} the number of laser active atoms per m³, n_{th}…thermal excitation of the lower laser level (important for quasi-three level systems like Yb:YAG, where the lower laser level has little energetic distance to the ground level and is therefore filled in thermal equilibrium according to the Boltzmann-statistics), Γ … laser mode overlap factor (He et al., 2006).
Neglecting all losses between laser gain medium and out-coupler the laser power P_l of the laser is given by

$$P_l = ½\, A\, c\, T_{out}\, E_{pl}\, P\,, \tag{7}$$

where A is the effective emitting area, T_{out} is the out-coupler transmission, and E_{pl} is the laser photon energy.

3.3 Simulating a Nd:YAG-rod-laser

Fig. 8 shows a very simple setup based on a side-pumped Nd:YAG-rod with diameter D = 3mm, length L_g = 75mm and dotation 1.1 at. %. Between the laser back mirror and the rod a SCPEM together with a PBSC (polarizing cube beam splitter) are placed. Pumping is done at 808nm, the laser emits at 1064nm.

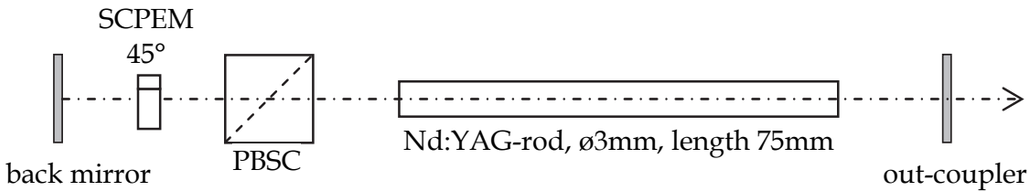

Fig. 8. Setup of a side-pumped DPSSL Q-switched with a SCPEM

The following parameters are used for the simulation:
resonator length L = 0.3m, maximum number of places for Nd-atomes in the YAG-host: 1.36 10^{28} m^{-3} → with dotation 1.1% the number of active atoms becomes n_{max} = 1.496 10^{26} m^{-3}, thermal population of lower laser level n_{th} = 0, out coupling surface $A = D^2\pi/4$, mode factor $\Gamma = L_g\ /(\ n_g\ L_g + L - L_g) = 0.2075$ [2], intrinsic cavity transmission T_c = 0.9 (taking into account the depolarizing effect of the laser rod, leading to high loss with the PBSC, further the PBSC-transmission is rated only >95%), out coupler transmission T_{out} = 0.1, life time of upper laser level t_n = 230µs, cross-section for stimulated emission σ = 28 10^{-24} m^{-3} (Koechner, 1999). ASE-factor M: to cause some amplification one spontaneously emitted photon must go after on laser-mirror-reflection through the whole laser rod. Hence M must be smaller than two

[2] This formula for the mode factor is obtained by assuming a constant laser mode cross-section A along the resonator, equal to the cross-section A of the gain. Further it must be considered that all generated photons are generated on the laser mode volume. A more detailed calculation needs a numerical integration over the photon density in the laser mode.

times the projection of a quarter of the effective out-coupling surface on the unit sphere in the gain medium $2(A/4)/(L/2)^2$ divided by the surface of the unit sphere 4π:

$$M < n_g^2 A/\pi/L^2/2 \sim 0.75\ 10^{-4} \tag{8}$$

This holds for loss free "perfect fitting" spontaneous emission from the centre of the laser cavity, which is never the case. We choose therefore a much smaller $M = 10^{-5}$ and remark that changing this figure has little influence on the results presented latter.
For the SCPEM the chosen parameters are $T_{min} = 0.01$, $T_{max} = 0.99$, first resonance frequency $f_R = 91$kHz, $\delta_1 = 1.2\,\pi$, $\delta_3 = 0$.
The absorbed pumping power is first assumed to be $P_{abs} = 100$W. By setting zero the left sides of the rate equations in Eq. 6 and using $T_{\max}$ for the SCPEM-transmission the stationary values of the laser power P_{l0} and the inversion n_0 can be calculated. The left graph in Fig. 9 shows this stationary laser output power P_{l0} versus the absorbed pumping power P_{abs}, the right graph in Fig. 9 shows the laser output power P_l versus the out-coupler transmission T_{out}.

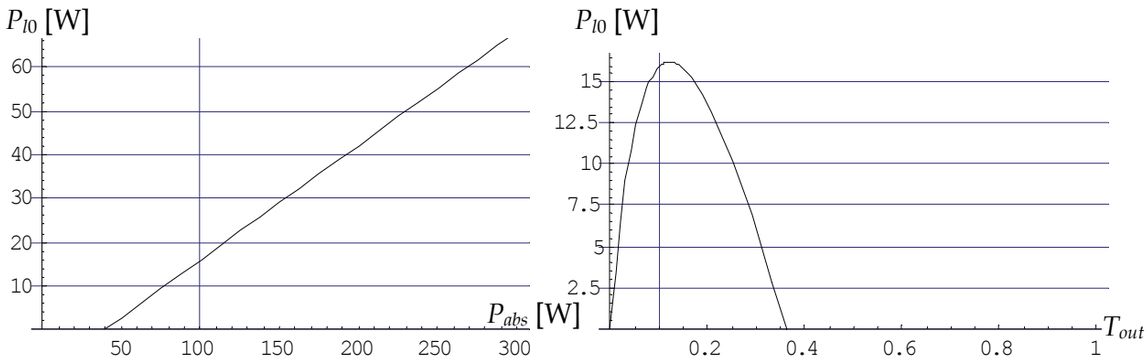

Fig. 9. cw-laser power versus P_{l0} pumping power P_{l0} (left); cw-laser power P_{l0} versus out-coupler transmission (right)

The vertical lines in Fig. 9 indicate the actual values of P_{abs} and T_{out} chosen in the simulation. Obviously the performance of this laser is poor due to the high loss in the cavity ($T_c = 0.9$).
Fig. 10 shows now the simulation result of Eq. 6 with the parameters given above.

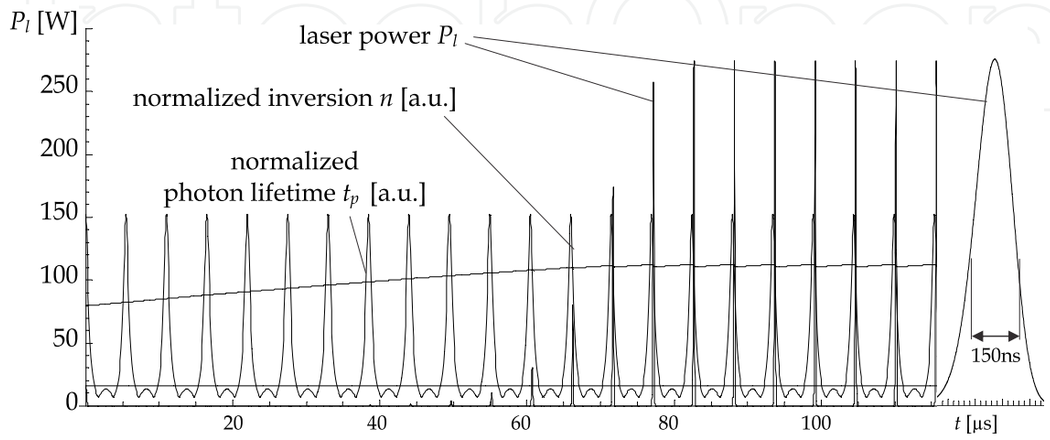

Fig. 10. Simulation results of Nd:YAG-rod laser based on Fig. 8 and Eq. 6.

The simulation starts with the steady state values for SCPEM-off. First the laser power drops to zero and remains zero during several SCPEM-cycles while the inversion n increases. Then pulsing starts and rapidly a quasi-stationary situation sets with constant pulsing at every transmission window with the following pulse parameters: peak power P_{peak} = 275W, FWHM-pulse duration t_{FWHM} = 150ns, pulse energy 46µJ, average power P_{av} = 8.44W. The poor average power is due to the fact that the pulses occur too late, shortly after the transmission peak, such that the laser-light is not polarized linearly and experience strong loss in the PBSC.

3.4 Chaotic behavior

Not every modulator frequency can be imposed to the laser. In many case chaotic behaviour is found, i.e. randomly varying pulse emission. Chaotic behaviour in connection with a SCPEM has interesting attractors in Poincare-maps (indicating deterministic chaos) and bifurcation diagrams showing that low modulator frequencies do not allow stable operation (Fig. 11).

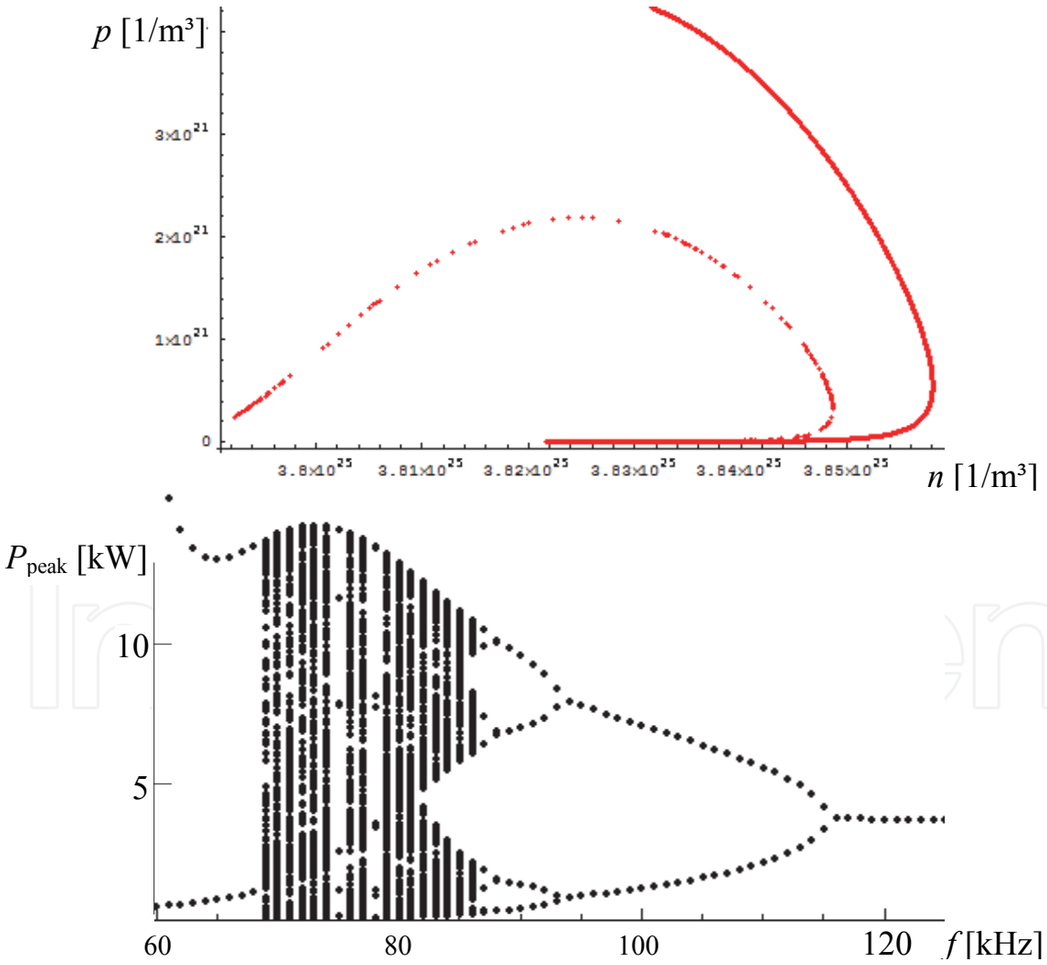

Fig. 11. Numerical analysis of a SCPEM-Q-switched Yb:YAG-slab laser
Poincare-map of photon density p vs. inversion density n for chaotic operation (top)
Bifurcation diagram: Peak powers P_{peak} vs. SCPEM-frequency f (bottom)

In Fig. 11 a side-pumped Yb:YAG-slab laser (slab size 10 x 5 x 0.5mm) with 50mm resonator length and 400W pumping power was simulated based on the rate equations 6.

3.5 Experimental results

Fig. 12 shows one setup that was used for a realization of SCPEM-Q-switching. The gain unit uses a Nd:YAG rod with diameter: 5 mm, length: 110 mm, doping concentration: 1.1% and polished ends (plano-plano ended) with an AR-coating for 1064 nm with reflection < 0.25%. It is side pumped from two sides with linear diode stacks, each one using 8 diode laser bars emitting at 808nm.

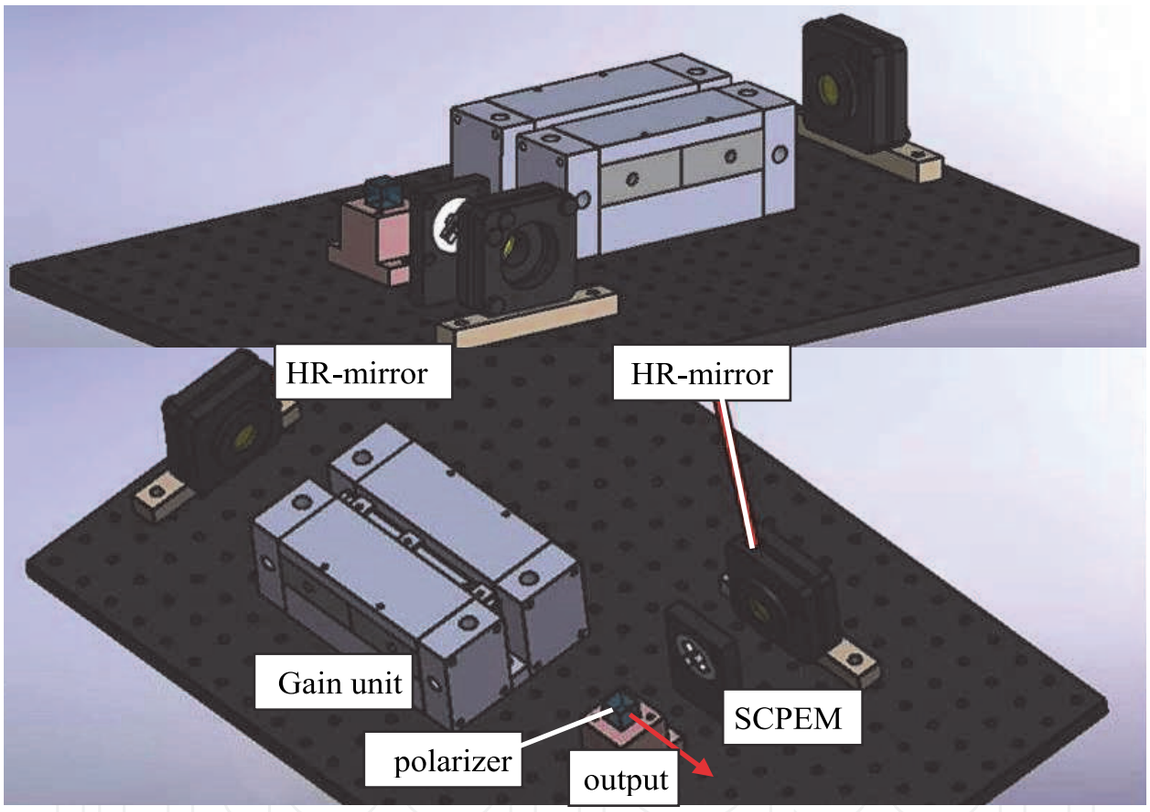

Fig. 12. Nd:YAG-laser for SCPEM-Q-switching

Fig. 13 shows stable pulsed operation with pulse frequency 190.2 kHz, average power 2.1 W, peak power 70 W, and pulse width 333ns. When the modulator is switched off the laser emits continuous wave with 2.8 W. This configuration, however do not allow stable operation at higher power. Fig. 14 shows the laser performance at higher power. The pulses are emitted irregularly with strongly varying pulse parameters.
Higher stable pulsed power can be achieved with a higher modulator frequency since low SCPEM-frequencies tend to produce chaotic output as indicated by Fig. 11.

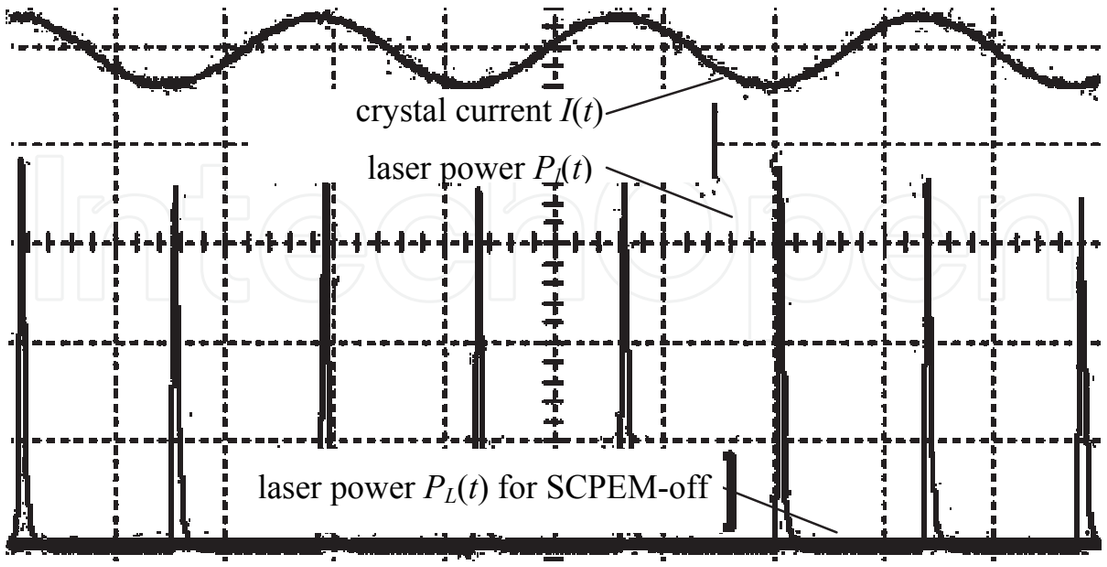

Fig. 13. Pulse sequence of a SCPEM-Q-switched Nd:YAG-laser: pulse frequency 190.2kHz, average power 2.1W, peak power 70W, pulse width 333ns. Crystal current $I(t)$ (upper graph) and laser powers $P_l(t)$ for SCPEM-on and SCPEM-off (with 2.8W cw-power)

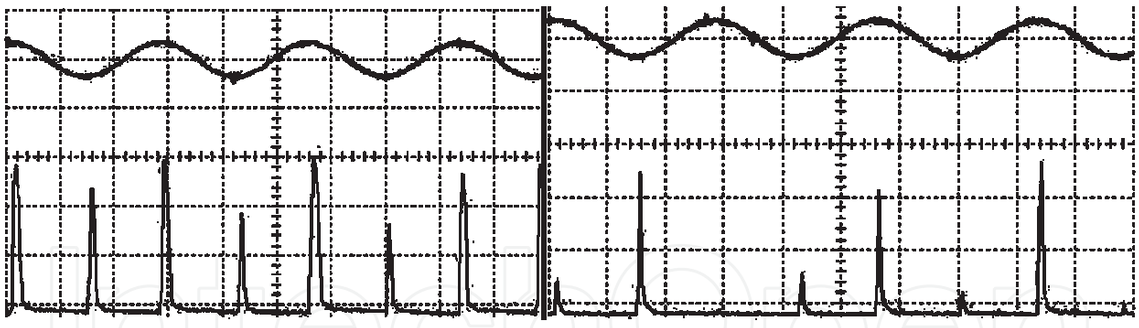

Fig. 14. Chaotic pulse sequences. Left: Average power 4.3 W (6 W with SCPEM-off). Right: Average power 6.5 W (9 W with SCPEM-off).

4. Conclusion

The possible use of SCPEMs for Q-switching was discussed. With a proper choice of parameters stable pulsed operation is possible with high efficiencies, little loss in average power, peak power 100 times higher then the average power, pulse repetition rates 100-300 kHz, and pulse durations down to 25ns. The important advantage is the simplicity of the solution making it interesting for quasi-cw applications, where no change of pulse repetition rate is needed. Especially frequency doubling and tripling should be possible with high efficiency with this type of laser operation.

5. Acknowledgment

This work was supported by the project "SCPEM-Laser" with the project number SPA/03-128 sponsored by the "Bundesministerium für Wissenschaft und Forschung" (Ministry for Science and Research).
Here we would like to thank Mr. Rok Petkovsek from the University of Ljubljana, who was involved in many realizations of SCPEM-Q-switching.

6. References

Badoz, J. & Canit, J.C. (1983). *New Design for a Photoelastic Modulator*, Appl. Opt. 22, 592

Bammer, F. & Holzinger, B. (2006). *A compact high brilliance diode laser*, SPIE-Proceeding of Photonics West 2006, High-Power Diode Laser Technology and Applications IV, Vol. 6104

Bammer, F.; Holzinger, B. & Schumi, T. (2006). *Time multiplexing of high power laser diodes with single crystal photo-elastic modulators*, Optics Express, Vol. 14, No. 8

Bammer, F. (2007). *Photoelastischer Modulator und Anwendungen*, Patent, AT 502 413

Bammer, F. & Holzinger, B. (2007). *Time-multiplexing generates a diode laser beam with high beam quality*, Optics and Laser Technology, 39, p. 1002 - 1007.

Bammer, F.; Holzinger, B. & Schumi, T. (2007). *A single crystal photo-elastic modulator*; SPIE-Proceeding of Photonics West 2007, Optical Components and Materials IV, Vol. 6469

Bammer, F. & Petkovsek, R. (2007). *Q-switching of a fiber laser with a single crystal photo-elastic modulator, Optics Express*, Vol. 15, No. 10

Bammer, F.; Petkovsek, R.; Frede, M. & Schulz, B. (2008). *Q-switching with a Dual Mode Single Crystal Photo-Elastic Modulator*, SPIE-Proceeding 7131, GCL/HPL 2008

Bammer, F.; Petelin, J.; Petkovšek, R. (2011). *Measurements on a Single Crystal Photo-Elastic Modulator*, OSA-Proceeding of CLEO2011

Bammer, F.; Schumi, T.; Petkovsek, R. (2011). *A new material for Single Crystal Modulators: BBO*, SPIE-Proceeding, 8080A-17, to be published

Bass, M. (1995). *Handbook of Optics*, McGraw Hill

Canit, J.C. & Pichon, C. (1984). *Low frequency photoelastic modulator*, App.Opt. 23/13, p.2198

Canit, C.; Gaignebet, E. & Yang, D. (1995). Photoelastic Modulator: *Polarization modulation and phase modulation*, J. Optics (Paris), vol. 26, n° 4, pp. 151-159

Dieulesaint, E. & Royer, D. (2000). *Elastic Waves in Solids*, Springer Publishing Company

Eichler, H.J. & Eichler, J. (2006). *Laser*, Springer Publishing Company

Halido, D. & Weil, R. (1974). *Resonant-piezoelectro-optic light modulation*, Journal of Applied Physics, Vol. 45, No. 5

Kemp, J.C. (1969). *Piezo-Optical Birefringence Modulators*, J. Opt. Soc. Am. 59, 950

Koechner, W. (1999). *Solid State Laser Engineering*, Springer Publishing Company

Krausz, F.; Kuti, Cs. & Turi, L. (1990). *Piezoelectrically Induced Diffraction Modulation of Light*, IEEE Journal of Quantum Electronics, Vol. 26, No. 7

Maldonado, T. A. (1995). Electro-optic modulators, Handbook of optics, McGraw-Hill

Nye, J. F. (1985). *Physical Properties of Crystals*, Oxford University Press

Petkovsek, R.; Saby, J.; Salin, F.; Schumi, T.; Bammer, F. (2011). *SCPEM-Q-switching of a fiber-rod-laser*, to be published

Schumi, T. (2006). *Analyse von photoelastischen Modulatoren aus Lithiumniobat*, Diploma Thesis, Vienna University of Technology

He, F., Price, J. H., Vu, K. T. et al. (2006). *Optimization of cascaded Yb fiber amplifier chains using numerical-modeling*, Optics Express 14, 12846-12858

Siegmann, A.E. (1986). *Lasers,* University Science Books, Mill Valley, California

Yariv, A. (1984). *Optical Waves in Crystals*, New York, Wiley

www.hindsinstruments.com

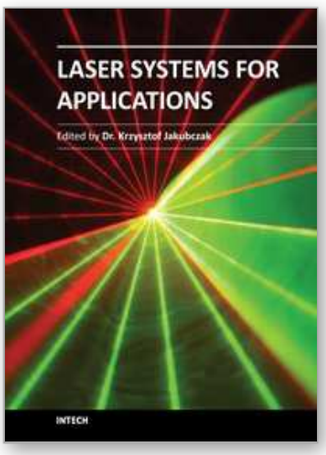

Laser Systems for Applications

Edited by Dr Krzysztof Jakubczak

ISBN 978-953-307-429-0
Hard cover, 308 pages
Publisher InTech
Published online 14, December, 2011
Published in print edition December, 2011

This book addresses topics related to various laser systems intended for the applications in science and various industries. Some of them are very recent achievements in laser physics (e.g. laser pulse cleaning), while others face their renaissance in industrial applications (e.g. CO2 lasers). This book has been divided into four different sections: (1) Laser and terahertz sources, (2) Laser beam manipulation, (3) Intense pulse propagation phenomena, and (4) Metrology. The book addresses such topics like: Q-switching, mode-locking, various laser systems, terahertz source driven by lasers, micro-lasers, fiber lasers, pulse and beam shaping techniques, pulse contrast metrology, and improvement techniques. This book is a great starting point for newcomers to laser physics.

InTech Europe
University Campus STeP Ri
Slavka Krautzeka 83/A
51000 Rijeka, Croatia
Phone: +385 (51) 770 447
Fax: +385 (51) 686 166
www.intechopen.com

InTech China
Unit 405, Office Block, Hotel Equatorial Shanghai
No.65, Yan An Road (West), Shanghai, 200040, China
中国上海市延安西路65号上海国际贵都大饭店办公楼405单元
Phone: +86-21-62489820
Fax: +86-21-62489821

IntechOpen